Progress In Electromagnetics Research C, Vol. 33, 55–66, 2012

COMPACT PRINTABLE ORIENTATION INDEPENDENT CHIPLESS RFID TAG

M. A. Islam*, Y. Yap, N. Karmakar, and A. Azad

Electrical and Computer Systems Engineering, Monash University, Building 72, Clayton, VIC 3800, Australia

Abstract—A novel design concept of a compact printable orientation independent chipless RFID tag is presented. The tag consists of a circular patch loaded with multiple slot ring resonators. This symmetric frequency domain based tag has the advantage to be read from any orientation with the reader antennas. The tag can be read in close proximity by chipless RFID tag reader with waveguide(s) and also can be read in both near field and far-field of the RFID tag reader with antennas. This tag does not have a ground plane and has higher data density compared to the existing printable chipless tags. The usability of this single sided tag in close proximity is verified by waveguide measurements for both proximity applications such as on ID access cards, item level tagging etc. and slot reading application such as on banknotes, credit cards etc.

1. INTRODUCTION

Radio Frequency Identification (RFID) is a wireless data capturing technology that uses radio frequency (RF) waves for extracting the encoded data from remotely placed tags. This system consists of two main elements, the RFID tag, where data is encoded, and the RFID reader, which is used for extracting the encoded data from the tags. The RFID tag has the potential to replace barcode, but it is still not used in low-cost applications because of its higher price compared to the barcode. The cost of the widely-used passive tags depends mainly on the chips used in them [1]. Therefore, research has been focused on developing chipless printable RFID tags.

Received 13 July 2012, Accepted 24 September 2012, Scheduled 28 September 2012
* Corresponding author: Md. Aminul Islam (aminul.islam@monash.edu).

A number of printable chipless RFID tags have been reported using simple or hybrid of time, frequency, phase domain and image-based encoding techniques. Among the time domain based tags, only SAW-based tags have the required data capacity [2], but the main drawback of this SAW tag is that it uses costly piezoelectric substrate. Moreover, using other printable techniques in time domain, it is not feasible to encode sufficient bits using microstrip delay lines [3] within a credit card sized area. Therefore, time domain-based tags cannot be used for high data density tag manufacturing. In phase domain-based tags only the tag using stub-loaded multiple patch antennas (SLMPA) [4] is printable and data is encoded in the cross-polarized backscattered phase. But if the backscattered phase is varied due to multipath, then it may cause bit encoding errors [5] and sufficient reliable phase resolution has not been achieved yet. Image-based tags are still in the experimental phase and need costly submicron-level printing.

If the frequency domain-based tag is considered, it is seen that these tags have higher data density than time-domain based tags. A 35-bit tag using spiral resonators and cross-polarized monopole antennas in the frequency domain has been presented in [6]. Low cost chipless RFID system for secure near-field data transfer is presented in [7] with a 9-bit tag having an area of a conventional ID card. It uses frequency shifting principle by length variation of the dipoles and complex higher order mode detection techniques. Another printable chipless tag was proposed in [8], where Multi-Resonant Dipole Antenna (MRDA) was attached to a monopole antenna to encode bits. But it requires both side printing alignment and number of dipoles increases linearly with the number of bits. Chipless tag using capacitively-tuned dipoles in [9] have problems with size and parasitic mutual coupling. Another printable tag using space filling curve [10] has difficulties in encoding data. Electromagnetic code is implemented in [11], where two Split Ring Resonators (SRRs) are used to encode each bit. A compact tag is proposed in [12] where frequency shifting technique is used by varying the length of coplanar strips. Another compact tag is proposed in [13, 14] using dual polarization technique to double the encoding capacity of the existing frequency domain based tags. Recently a chipless RFID tag based on dual-band resonators is presented in [15] with a calibration technique to increase the read range in frequency domain based RFID tags.

However, all the frequency domain based tags described above have a common drawback, that they are needed to be aligned with the linearly polarized reader antennas. Circularly polarized UWB reader antennas are required to overcome the misalignment problem.

But circularly polarized antennas usually have lower bandwidth which decreases the encoding capacity of the frequency domain based tags. If a compact fully-printable orientation independent linearly polarized tag with sufficient data capacity can be developed, it will gain wide acceptance in many passive chipless RFID tag applications.

In this paper, a novel compact easily-printable slot ring resonator loaded chipless RFID tag is proposed to overcome the limitations of the other chipless tags suggested in the previous studies such as printing complexities using conductive ink due to the alignment mismatch between tag's two sides, total tag area, manufacturing cost and orientation dependency. Like most other designs, the size of our tag will not increase linearly with the number of bits as the bit representing slots will be cut inside the patches. More importantly, this symmetric tag is independent of rotation around orthogonal axis with the reader antenna and it does not require a ground plane like most other proposed chipless tags. Hence, this orientation independent single sided tag can be used in ID or credit cards, tickets, banknotes and also can be directly printed on paper or plastic packets for item-level tagging.

Rest of the paper is organized as follows: Section 2 presents the related theory and operating principle of the proposed chipless RFID tag. Section 3 presents the design of the tag. Section 4 presents the simulation and experimental measurement results followed by conclusion in Section 5.

2. THEORY OF OPERATION

2.1. Slot Ring Resonators

Slot ring resonators of different diameters are used to create different frequency signatures for this tag, where each signature is used to represent one bit. It has two main advantages over other resonant structures. Firstly, resonances at the 2nd, 3rd and other harmonics are not present in the backscattered signal from a slot ring resonator loaded patch. Due to the ring resonator's symmetric and continuous structure, even and odd harmonics current path cannot be created and hence they are not appearing in the backscattered signal (Figure 1). So we can encode data using the whole UWB band (3.1 to 10.6 GHz), as the 2nd and 3rd harmonic for the 3.1 GHz resonant slot will not appear at 6.2 GHz and 9.3 GHz for the slot ring resonators and so on.

Secondly, due to its symmetric structure we will get same frequency signature at any orientation of the ring resonator with the reader antenna. Hence we can have an orientation independent tag using this slot ring resonators.

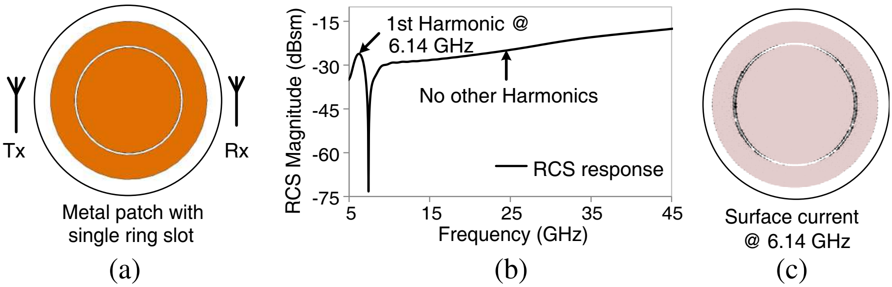

Figure 1. Backscattered frequency response and surface current plot of a slot ring-resonator inside a patch.

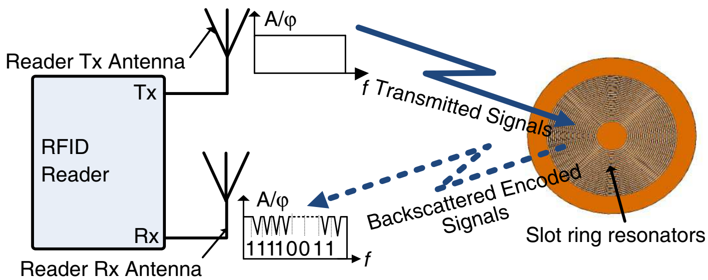

Figure 2. Working principle of the proposed chipless RFID tag.

2.2. Working Principle of the Proposed Tag

The working principle is shown in Figure 2. The tag is excited by a linearly-polarized transmitter antenna (Tx) and the frequency encoded backscattered signal from the tag is received by another linearly-polarized receiver antenna (Rx). Since the tag is symmetrical to the reader antenna, the backscattered encoded frequency signature is independent of the orientation of the tag.

3. CHIPLESS RFID TAG DESIGN

The proposed tag was designed and simulated in CST Microwave Studio 2011 and the simulation setup is shown in Figure 3. Linearly-polarized plane wave is used for the excitation of the tag and E-field (far-field) probes and RCS probes are placed 50 mm away from the tag to receive the far-field backscattered signal from the tag.

The layout of an N-bit orientation independent slot ring resonator loaded tag is shown in Figure 4 with dimensions as parameters. Where R_{patch} is the radius of the patch, R_1 is the radius of the longest ring resonator and R_n is the radius of the shortest ring resonator, S_s is the separation between the resonators, W_s is the width of the slot

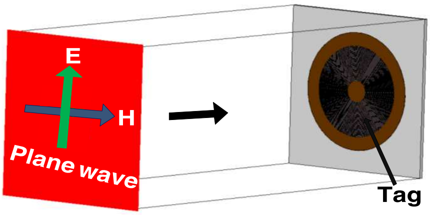

Figure 3. Simulation setup for the slot ring resonator loaded chipless tag.

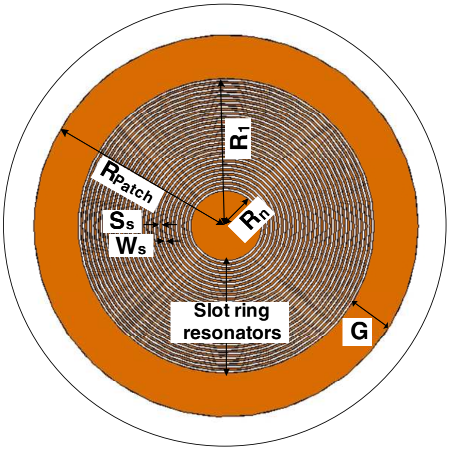

Figure 4. N-bit orientation independent slot ring resonator loaded tag.

resonators, and G is the gap between the edge of the patch and longest resonator. In order to keep the design simple and easily-printable, we kept W_s and S_s the same for every ring resonator. The rings are numbered according to their lengths and ring number 1 is the longest one with the lowest frequency, which is denoted as MSB. Ring number 'n' with the highest frequency is denoted as LSB.

When a plane wave excites this slot ring resonator loaded patch, it shows a frequency selective behavior with peaks followed by deep notches at the resonant frequencies of the ring resonators. We can increase the number of bits by increasing the number of ring resonators within the patch. We can change the logic state of a bit simply by removing the slot ring resonator which will remove the resonant frequency of the slot. The removal of notch frequency is denoted as logic '0' where the appearance of a notch is denoted as logic '1'.

The proposed tag can be directly printed on the paper or plastic packets of the items, and also can be inserted inside ID cards. The resonant frequencies are needed to be recalculated or radius of the slot ring resonators are needed to be readjusted to get resonances at some fixed values based on the different thickness (h) and permittivity (ε_r) of the substrates [14]. The resonant frequency decreases with the increment in the substrate thickness and permittivity. In case of ID cards, the resonant frequencies and effective permittivity will be determined by (1) and (2).

$$f = \frac{c}{2L}\sqrt{[2/\{\varepsilon_{r(\text{substrate})} + \varepsilon_{r(\text{superstrate})}\}]} \tag{1}$$

$$\varepsilon_{r(\text{substrate})} = \frac{(d_1 + d_2) * \varepsilon_{r(\text{substrate1})} * \varepsilon_{r(\text{substrate2})}}{d_2 * \varepsilon_{r(\text{substrate1})} + d_1 * \varepsilon_{r(\text{substrate2})}} \tag{2}$$

Hence, after the characterization of the substrate we can modify our design for that particular item type to obtain resonance at particular frequencies, which can be read by a single reader worldwide. Thus our design can be used like a barcode for item-level tagging.

4. RESULTS

4.1. Simulation Results of the Proposed Tag

For proving the design concept, we started with a circular metallic patch loaded with eight slot ring resonators as shown in Figure 5(a). The dimensions of the tag are chosen as $W_s = 0.2$ mm, $S_s = 0.2$ mm, $R_{\text{patch}} = 7.8$ mm, $R_1 = 5.8$ mm and $R_n = 2.8$ mm and $G = 2$ mm.

To facilitate in-house fabrication and near-field measurement, we chose the minimum dimension as 0.2 mm and operating frequency band as 6 to 13 GHz respectively. Tags with different bit combinations as shown in Figure 5 were simulated and milled on Taconic TLX-9 (permittivity, $\varepsilon_r = 2.5$, thickness, $h = 0.5$ mm, loss tangent, $\tan\delta = 0.0019$).

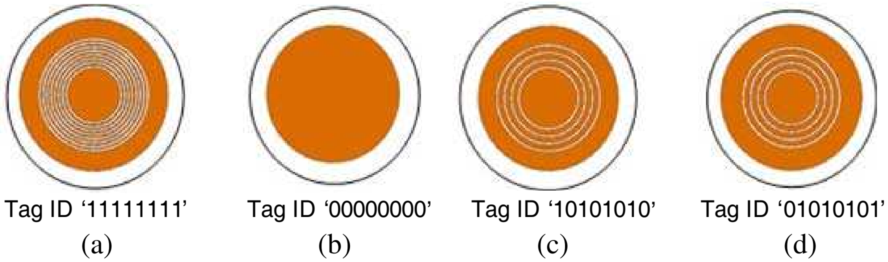

Figure 5. Layout of the simulated tags with different IDs. (a) '11111111', (b) '00000000', (c) '10101010', and (d) '01010101'.

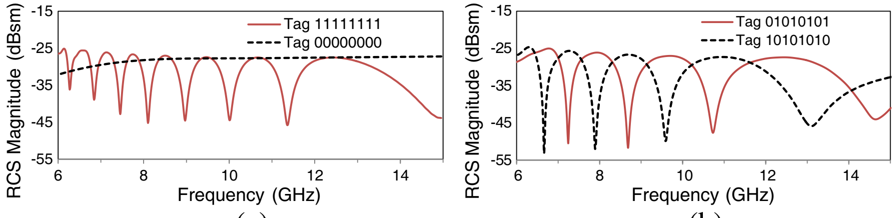

Figure 6. Simulation results for the tags with different IDs of Figure 5. (a) Tag IDs '11111111' and '00000000' and (b) Tag IDs '10101010' and '01010101'.

The simulation results are shown in Figure 6. In Figure 5(a) the 8-bit tag has all 1's. Eight frequency signatures are present in the backscattered signal from the tag, which is used to encode eight bits. The simulation result is shown in Figure 6(a). All 8 slots are removed as shown in Figure 5(b) to get the tag with all 0's and the simulation result is shown in Figure 6(a) where all the frequency signatures are removed compared to all 1's. Later tags with IDs '10101010' and '01010101' as shown in Figures 5(c) and (d) are simulated and the results are shown in Figure 6(b). It is observed that the corresponding frequencies of 0's are removed in the backscattered signal from the tags. The resonant bit positions are represented by the peaks, which are followed by dips in the frequency response from the tag. The changes in the peak positions (not the dips) due to the removal of the slots are negligible for all the bit combinations. Moreover, these very little shifts in the adjacent frequency peaks after the removal of the slots can be overcome by simple signal processing.

4.2. Measurement Techniques

The tag can be read in both near-field and far-field of the reader antennas by placing two linearly-polarized antennas on the same side of the tag; one as a transmitter and the other one as a receiver and measuring the S_{21}. Based on its different applications, the tag can also be measured by placing the transmitter antenna in front of the tag and the receiver antenna behind the tag as it has no ground plane, which is shown in Figure 7.

Different applications like the proximity cards (access control cards, public transport fare cards etc.) and other secure paper documents can be detected by placing it just in front of the waveguide-based reader and measuring the return loss (S_{11}) at port 1 (Figure 8(a)).

Credit cards and banknotes can be read by inserting them in a slot cut inside a waveguide and measuring insertion loss (S_{21})

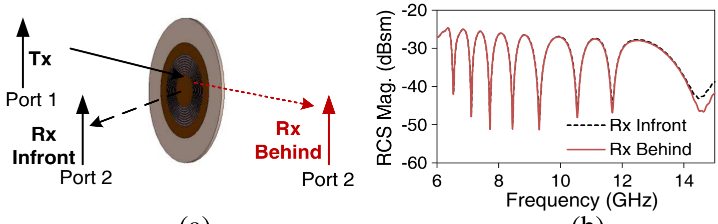

Figure 7. (a) Simulation setup with receiver antenna probes in-front and behind of an eight bit tag and (b) simulation results.

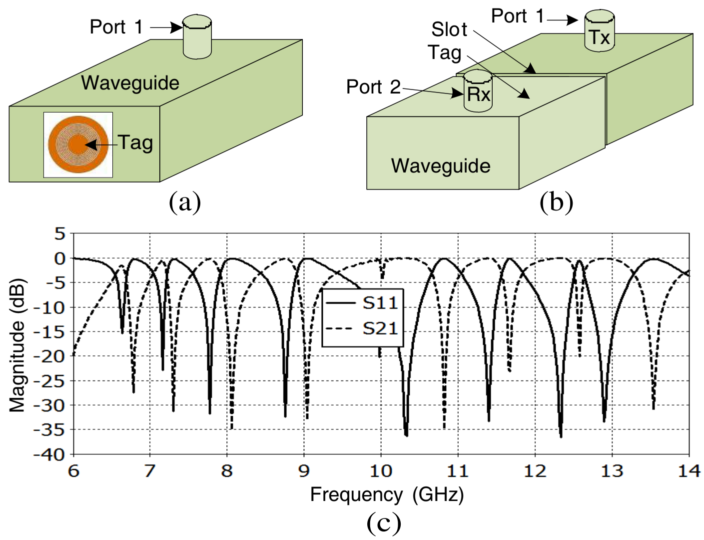

Figure 8. (a) Proximity, (b) slot card measurement setups and (c) simulation results.

(Figure 8(b)) of the two ports as described in [16]. The simulation result for proximity and slot card reading using waveguide is shown in Figure 8(c). The design concept of obtaining response from multiple slot ring resonators is verified by the both proximity and slot card waveguide measurement setup techniques.

Tags with four different IDs as shown in Figure 9 have been fabricated to obtain measurement result for proving the design concept used in simulation.

4.3. Proximity Waveguide Measurement Results

The measurement setup is shown in Figure 8(a). The tag is placed in front of the linearly-polarized waveguide with fundamental mode

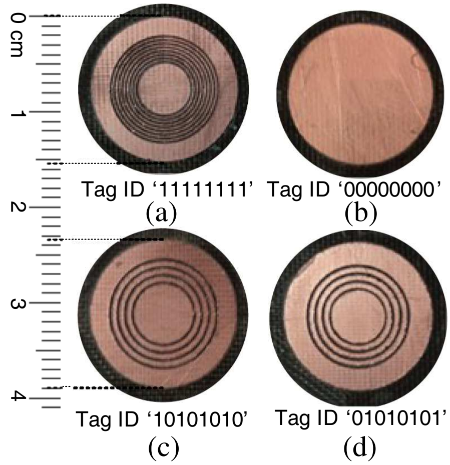

Figure 9. Photograph of the fabricated tags with different IDs (a) '11111111', (b) '00000000', (c) '10101010', and (d) '01010101' on Taconic TLX-9 ($\varepsilon_r = 2.5$, $h = 0.5\,\text{mm}$, $\tan\delta = 0.0019$).

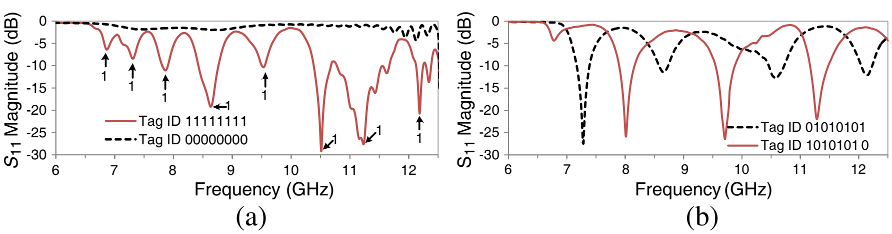

Figure 10. Measured return losses (S_{11}) for the tags with (a) IDs '11111111' and '00000000' and (b) IDs '10101010' and '01010101'.

bandwidth of 6–13 GHz and return loss is measured using the Agilent PNA E8361A vector network analyzer. The measured S_{11} results are shown in Figures 10(a) and (b) to show the frequency response of the designed tag. In Figure 10(a) the curves are showing results for the tags with IDs '11111111' and '00000000'. Eight dips are seen in the magnitude response for eight 1's of the tag with ID 11111111, but no dips for the eight 0's in the magnitude response for the tag with ID '00000000'. Few small notches are observed due to noise in the frequency response of Figure 10(a). Several designs and tag detection algorithms have already been proposed in literature on chipless RFID tag reader to detect the tag avoiding notches created by noise [17, 18] and also to incearse the reading range of the tag upto 2 meters [19]. As the notch positions of the bits will be known beforehand, hence the notches due to noise at other points can be avoided easily in the reader detection algorithm. But notches at the bit positions

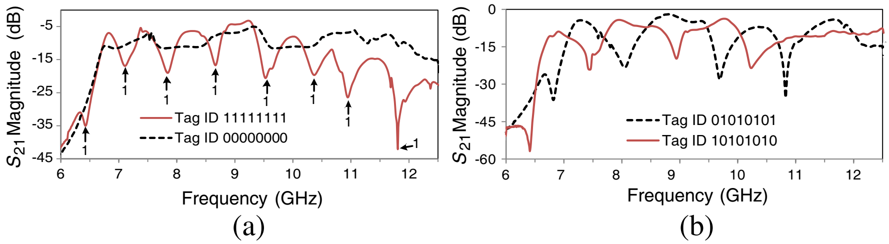

Figure 11. Measured insertion losses (S_{21}) for the tags with (a) IDs '11111111' and '00000000' and (b) IDs '10101010' and '01010101'.

can be differentiated by putting some boundary conditions and signal processing in the reader detection algorithm [18]. The measured S_{11} magnitudes for the tags with IDs '10101010' and '01010101' are shown in Figure 10(b). Here we can see four dips for each tag at the corresponding positions of four 1's in their IDs.

4.4. Slot Card Waveguide Measurement Results

The measurement setup is shown in Figure 8(b). Where the tag is placed inside a slot of the linearly polarized waveguide and insertion loss (S_{21}) is measured using the network analyzer. The measured S_{21} magnitudes for different tags are shown in Figures 11(a) and (b).

In Figure 11(a) the curves are showing results for the tags with IDs '11111111' and '00000000'. Eight dips are seen in the magnitude response for eight 1's of the tag with ID 11111111, but no dips for the eight 0's in the magnitude response for the tag with ID '00000000'. The measured S_{21} magnitudes for the tags with IDs '10101010' and '01010101' are shown in Figure 11(b). Here we can see four dips for each tag at the corresponding positions of four 1's in their IDs.

The main concept for this tag is obtaining similar results for all orientation of the tag loaded with slot ring resonators which have been proved from the measured results.

5. CONCLUSION

A novel compact chipless RFID tag concept is presented here, which uses slot ring resonators to create frequency signatures in the backscattered signal. This tag is symmetric and hence independent of orientation with its reader. The concept has been proved from the simulation and proximity measurement results using waveguides for a 8-bit prototype. This single sided, compact and orientation independent tag has a great potential to be used in millions both for identification and authentication. It can be printed directly on the items like barcode using conductive ink. Tags with higher number of bits can be used for identification in many products like ID or credit cards, grocery items, library books in both near and far-field measurement from the reader. On the other hand, tags with lower number of bits can be used for authentication in banknotes and paper documents in proximity measurements with higher accuracy and security. In future research, study on increasing the encoding capacity and parameter optimization of this tag design, improving the directly conductive ink printed tag performance on items and near and far-field measurement comparison with simulation results will be carried out.

REFERENCES

1. Kaiser, U. and W. Steinhagen, "A low-power transponder IC for high-performance identification systems," *IEEE Journal of Solid-State Circuits*, Vol. 30, No. 3, 306–310, Mar. 1995.
2. Hartmann, C. S., "A global SAW ID tag with large data capacity," *IEEE Ultrasonics Symp.*, 65–69, 2002.
3. Botao, S., C. Qiang, Y. Amin, D. S. Mendoza, L. Ran, and Z. Li-Rong, "An ultra-low-cost RFID tag with 1.67 Gbps data rate by ink-jet printing on paper substrate," *IEEE Asian Solid State Circuit. Conf.*, 2010.
4. Balbin, I. and N. C. Karmakar, "Phase-encoded chipless RFID transponder for large-scale low-cost applications," *IEEE Microwave and Wireless Components Letters*, Vol. 19, 509–511, 2009.
5. Mukherjee, S., "Chipless radio frequency identification by remote measurement of complex impedance," *European Conference on Wireless Technologies*, 249–252, Oct. 8–10, 2007.
6. Preradovic, S. and N. C. Karmakar, "Design of fully printable planar chipless RFID transponder with 35-bit data capacity," *European Microwave Conference (EuMC)*, 013–016, Sept.–Oct. 2009.
7. Deepu, V., A. Vena, E. Perret, and S. Tedjini, "New RF identification technology for secure applications," *IEEE Int. Conf. on RFID-Technology and Applications (RFID-TA)*, 159–163, Jun. 17–19, 2010.
8. Balbin, I. and N. Karmakar, "Novel chipless RFID tag for conveyor belt tracking using multi-resonant dipole antenna," *European Microwave Conference (EuMC)*, 1109–1112, Sept. 29–Oct. 1, 2009.
9. Jalaly, I. and I. D. Robertson, "Capacitively-tuned split microstrip

resonators for RFID barcodes," *European Microwave Conference*, Vol. 2, 4, Oct. 4–6, 2005.

10. McVay, J., A. Hoorfar, and N. Engheta, "Space-filling curve RFID tags," *IEEE Radio and Wireless Symposium*, 199–202, Jan. 17–19, 2006.
11. Hyeong-Seok, J., L. Won-Gyu, O. Kyoung-Sub, M. Seong-Mo, and Y. Jong-Won, "Design of low-cost chipless system using printable chipless tag with electromagnetic code," *IEEE Microwave and Wireless Components Letters*, Vol. 20, 640–642, 2010.
12. Vena, A., E. Perret, and S. Tedjini, "Novel compact RFID chipless tag," *PIERS Proceedings*, 1062–1066, Morocco, Mar. 20–23, 2011.
13. Aminul Islam, M. and N. Karmakar, "Design of a 16-bit ultra-low cost fully printable slot-loaded dual-polarized chipless RFID tag," *Asia-Pacific Microwave Conference Proceedings (APMC)*, 1482–1485, Dec. 5–8, 2011.
14. Islam, M. A. and N. C. Karmakar, "A novel compact printable dual-polarized chipless RFID system," *IEEE Transactions on Microwave Theory and Techniques*, Vol. 60, 2142–2151, 2012.
15. Girbau, D., J. Lorenzo, A. Lazaro, C. Ferrater, and R. Villarino, "Frequency-coded chipless RFID tag based on dual-band resonators," *IEEE Antennas and Wireless Propagation Letters*, Vol. 11, 126–128, 2012.
16. Aminul Islam, M., M. Shakil Bhuiyan, and N. Karmakar, "A novel compact chipless RFID tag and near-field reader," *Asia-Pacific Microwave Conference Proceedings (APMC)*, 1518–1521, Dec. 5–8, 2011.
17. Kalansuriya, P., N. Karmakar, and E. Viterbo, "Signal space representation of chipless RFID tag frequency signatures," *IEEE Global Telecommunications Conference (GLOBECOM)*, 1–5, 2011.
18. Koswatta, R. and N. C. Karmakar, "Moving average filtering technique for signal processing in digital section of UWB chipless RFID reader," *Asia-Pacific Microwave Conference Proceedings (APMC)*, 1304–1307, Dec. 5–8, 2010.
19. Lazaro, A., A. Ramos, D. Girbau, and R. Villarino, "Chipless UWB RFID tag detection using continuous wavelet transform," *IEEE Antennas and Wireless Propagation Letters*, Vol. 10, 520–523, 2011.